

Polarons in Carbon Nanotubes

M. Verissimo-Alves¹, R. B. Capaz¹, Belita Koiller¹, Emilio Artacho², and H. Chacham³

¹*Instituto de Física, Universidade Federal do Rio de Janeiro, Caixa Postal 68528, Rio de Janeiro, RJ, Brazil, 21945-970*

²*Departamento de Física de la Matéria Condensada, C-III and Instituto Nicolás Cabrera, Universidad Autónoma de Madrid, 28049 Madrid, Spain*

³*Departamento de Física, ICEx, Universidade Federal de Minas Gerais, Caixa Postal 702, 30123-970 Belo Horizonte, MG, Brazil*

(October 25, 2018)

Abstract

We use *ab initio* total-energy calculations to predict the existence of polarons

Carbon nanotubes (CNTs) have recently attracted a great deal of interest for their unusual electronic and mechanical properties [1]. In this context, the interplay between mechanical distortions and electronic structure plays a central role. Mechanical distortions can be generally classified as externally applied or spontaneous. Effects of externally applied distortions such as twisting, bending and axial compression of CNTs on their electronic structure have been the subject of many studies [2,3,4,5]. Spontaneous distortions are usually related to strong electron-phonon interactions, and classic examples are polaron formation in ionic solids [7], Peierls distortion in 1D metals [8] and related excitations (solitons and polarons) in conjugated polymers [9]. Symmetry-breaking distortions in fullerenes and CNTs have also been considered by several authors [10,11,12,13,14,15].

In this work we show that an extra electron or hole in a CNT causes a completely different kind of spontaneous distortion: a combined radial (breathing-mode-like) and axial distortion. This perturbation causes the band edge energies to vary linearly and the elastic energy to increase quadratically with the distortion parameters. Therefore, the total energy of the system has a minimum at a nonzero value of the distortion parameter and a polaron is formed.

The distortions considered here are changes in the CNT radius and length, characterized by the radial and axial strain parameters

$$\epsilon_r = \frac{(R - R_0)}{R_0} \text{ and } \epsilon_z = \frac{(l - l_0)}{l_0}, \quad (1)$$

respectively, where R_0 is the equilibrium radius for a neutral, undistorted CNT and l_0 is the equilibrium length of its unit cell. Consider a semiconducting CNT with a single extra electron at the bottom of the conduction band. Allowing $\epsilon_{r,z}$ to depend on z , the CNT axis direction, we write the change in total energy caused by this extra electron as [16]:

$$\begin{aligned} E = & -\frac{\hbar^2}{2m_{eff}} \int_{-\infty}^{+\infty} \psi^*(z) \frac{d^2}{dz^2} \psi(z) dz \\ & + \lambda_r \int_{-\infty}^{+\infty} \psi^*(z) \psi(z) \epsilon_r(z) dz \\ & + \lambda_z \int_{-\infty}^{+\infty} \psi^*(z) \psi(z) \epsilon_z(z) dz \end{aligned}$$

$$\begin{aligned}
& + \frac{k_r}{2} \int_{-\infty}^{+\infty} \epsilon_r^2(z) dz + \frac{k_z}{2} \int_{-\infty}^{+\infty} \epsilon_z^2(z) dz \\
& + k_{rz} \int_{-\infty}^{+\infty} \epsilon_r(z) \epsilon_z(z) dz,
\end{aligned} \tag{2}$$

where $\psi(z)$ is the electronic wavefunction and m_{eff} is the electron effective mass; $k_{r,z}$ and $\lambda_{r,z}$ are the effective spring constants per unit length and the electron-phonon coupling constants relative to the purely radial (r) and purely axial (z) strains; k_{rz} is the spring constant relative to coupled radial and axial strains. Minimizing (2) with respect to ψ^* and $\epsilon_{r,z}$ leads to the following expressions for the axial and radial strains:

$$\epsilon_{r,z} = \frac{\lambda_{z,r} k_{rz} - \lambda_{r,z} k_{z,r}}{k_r k_z - k_{rz}^2} \psi^* \psi = C_{r,z} \psi^* \psi \tag{3}$$

and to the nonlinear Schrödinger equation

$$\left[\frac{d^2}{dz^2} - \tilde{C} \psi^*(z) \psi(z) \right] \psi(z) = \tilde{\varepsilon} \psi(z) \tag{4}$$

with $\tilde{C} = (2m_{eff}/\hbar^2)(\lambda_r C_r + \lambda_z C_z)$. Eq. (4) admits the following bound normalized solution:

$$\psi(z) = \sqrt{\frac{a}{2}} \operatorname{sech}(az), \tag{5}$$

where the inverse polaron length, a , and its binding energy, $\varepsilon = -\hbar^2 \tilde{\varepsilon} / 2m_{eff}$, are given by

$$a = \frac{\tilde{C}}{4} ; \quad \varepsilon = -\frac{\hbar^2}{2m_{eff}} \frac{\tilde{C}^2}{16}. \tag{6}$$

The resulting maximum axial and radial distortions are $\epsilon_{r,z}^{max} = aC_{r,z}/2$.

The polaron mass can be estimated using a semi-classical description of the electron motion. Assuming that the polaron propagates with velocity v_{pol} without changing its characteristic shape, we write the total kinetic energy of the electron-lattice system as the sum of the energy of an electron propagating in the conduction band with velocity v_{pol} plus the kinetic energy of the ions due to the propagation of the polaron:

$$T_{pol} = T_e + T_{ions} = \frac{1}{2} m_{eff} v_{pol}^2 + T_{ions} = \frac{1}{2} m_{pol} v_{pol}^2. \tag{7}$$

Both radial and axial components of the ionic velocities contribute to the ionic kinetic energy:

$$\begin{aligned}
T_{ions} &= \frac{1}{2} \sum_{ions} M_i \left[R_0^2 \left(\frac{\partial \epsilon_r}{\partial t} \right)^2 + \frac{2}{0} \left(\frac{\partial \epsilon_z}{\partial t} \right)^2 \right] \\
&= \frac{1}{2} \sigma v_{pol}^2 \int_{-\infty}^{+\infty} dz \left[R_0^2 \left(\frac{\partial \epsilon_r}{\partial z} \right)^2 + \frac{2}{0} \left(\frac{\partial \epsilon_z}{\partial z} \right)^2 \right]
\end{aligned} \tag{8}$$

where M_i is the ionic mass and σ is the linear mass density of the CNT. Using Eqs. (3) and (5), we obtain the polaron mass:

$$\frac{m_{pol}}{m_{eff}} = 1 + \frac{2\sigma a \tilde{C}^2}{15m_{eff}} \left[\left(\frac{R_0 C_r}{2} \right)^2 + \left(\frac{{}_0 C_z}{2} \right)^2 \right] \tag{9}$$

Exactly the same results are obtained for an extra hole in the valence band, with a reversed sign in the definition of λ , as discussed below. All quantities defined above are functions only of $k_{r,z,rz}$, $\lambda_{r,z}$, m_{eff} , R_0 , ${}_0$ and σ . We determine R_0 , ${}_0$ and σ from the CNT optimized geometry, and m_{eff} is taken from tight-binding (TB) calculations [1] with a hopping parameter of $\gamma_0 = -3.03$ eV.

We obtain $k_{r,z,rz}$ and $\lambda_{r,z}$ from *ab initio* calculations. Our calculations are performed using the SIESTA [17] code, a numerical-atomic-orbital method based on density functional theory. This technique has been successfully applied to a number of studies involving nanotubes [5,18]. We use a generalized gradient approximation for exchange and correlation and norm conserving pseudopotentials. A split-valence double- ζ basis of pseudoatomic orbitals with an orbital confining energy of 0.3 eV and an energy cutoff of 300 Ry for the fast Fourier transform integration mesh are used. In order to probe the dependence of polaron properties on CNT geometry, we perform calculations for (11,0) and (7,0) zigzag nanotubes. These are within the range of recently reported experimental values for nanotube diameters [19]. The k-point sampling is composed of six k-points in the CNT axis direction, which allows us to use a minimal hexagonal supercell of 44 atoms for a (11,0) CNT and 28 atoms for a (7,0) CNT. The in-plane lattice parameter was chosen to be large enough (30 Å) to ensure that there is negligible interaction between periodic CNT images.

The calculations are performed for uniformly distorted neutral CNTs. Then ϵ_r and ϵ_z become independent of z and the change in total energy per unit cell can be written as

$$\Delta E_{tot} = 0 \left(\frac{1}{2} k_r \epsilon_r^2 + \frac{1}{2} k_z \epsilon_z^2 + k_{rz} \epsilon_r \epsilon_z \right). \quad (10)$$

We vary the CNT radius while keeping $\epsilon_z = 0$, and we vary the CNT unit cell length while keeping $\epsilon_r = 0$: k_r and k_z are obtained, respectively, from the curvature on the ΔE_{tot} vs. $\epsilon_{r,z}$ plots, as shown in Fig. 1(a) for the (7,0) CNT and in Fig. 1 (b) for the (11,0) CNT. Then, by relaxing the unit cell length for a given nonzero value of the radial strain ϵ_r , k_{rz} is obtained. The resulting values for k_r , k_z and k_{rz} for both (11,0) and (7,0) CNTs are shown in Table I.

The electron-phonon coupling constants for electrons (holes), $\lambda_{r,z}^{e(h)}$, are obtained from the linear variation in the conduction (valence) band edge energies for a given strain energy $\epsilon_{r,z}$:

$$\Delta E_{r,z}^{e(h)} = \pm \lambda_{r,z}^{e(h)} \epsilon_{r,z}, \quad (11)$$

where the positive sign is for electrons and the negative sign is for holes. Plots for $\Delta E_{r,z}^{e(h)}$ for both (11,0) and (7,0) CNTs are shown in Figs. 2(a) and (b), respectively. Values for all electron-phonon coupling constants are displayed in Table I.

The calculated polaron signatures (lengths, binding energies, masses and maximum distortions) calculated from the *ab initio* elastic and electron-phonon constants are also presented in Table I. The differences between the results for the (11,0) and (7,0) tubes allow us to anticipate a rich dependence on the CNT's diameter and chirality. This dependence can be understood as a superposition of two contributions: a "classical" and a "quantum" contribution. The "classical" contribution comes simply from the dependence of the elastic constants on the CNT's diameter. From Table I, one sees that all elastic constants are smaller for the thinner (7,0) CNT. This effect can be understood in simple terms by considering CNTs with different diameters where the same percentual radial distortion is applied. Each bond in the CNTs' zigzag chains will be deformed by the same amount, but the thinner CNTs have less bonds along the chain. Considering the elastic energy to be proportional to the number of deformed bonds, the thinner CNTs will have smaller k 's. A similar argument

applies to the axial elastic constants. So, considering this “classical” argument alone, one would expect stronger polaron signatures for thinner CNTs.

The “quantum” contribution comes from the different possible signs and magnitudes of the electron-phonon coupling constants $\lambda_{r,z}^{e(h)}$. As one sees from Table I, it is difficult to identify simple trends of the λ 's with geometry. Simpler TB models predict a constant value of λ for zig-zag tubes under uniaxial strain [3]. This is probably an effect of curvature and rehybridization of $\sigma - \pi$ orbitals [20] in small-diameter CNTs, which are generally neglected in TB calculations.

Analysis of polaron signatures in Table I might suggest that the observation of polarons in CNTs would be very difficult. Although we have not attempted to reach particular combinations of chirality and carrier type to achieve the strongest polaron signatures, the studied examples yield binding energies at most $\simeq 0.3$ meV, and the largest polaron mass $\simeq 0.2\%$ larger than the free electron mass for the hole polaron in the (7,0) CNT.

However, these are signatures for a *single* polaron. The situation changes completely when we consider *collective* polaron effects. One example is the CNT length variation due to polarons. The total length variation on an CNT caused by the presence of a single polaron is:

$$\Delta^{(1)} = \int_{-\infty}^{\infty} dz \epsilon_z(z) = C_z \quad (12)$$

For the hole polaron in the (7,0) CNT, $C_z = 0.02$ Å. Therefore, a modest number of 500 polarons would cause a sizeable 10 Å variation in the nanotube length, large enough to be observed, for instance, in AFM or STM experiments where CNTs are used as probes. A related quantity is the strain- charge coefficient (SCC) [21],

$$\frac{\Delta /}{\Delta y} = \frac{N\Delta^{(1)}}{0} = \frac{NC_z}{0}, \quad (13)$$

where $\Delta /$ is the fractional change in length caused by a Δy change in the concentration of injected charge per carbon atom and N is the number of atoms in the unit cell. Our calculated values for the SCC are also presented in Table I. They are comparable to the

experimentally measured values of 0.17 (for low charge injection) in the context of electro-mechanical actuation in CNTs [21]. This suggests that polaron formation may contribute significantly to the observed actuation, although it may not be the only driving mechanism, since experiments are usually undertaken in much more complex environments where inter-tube interactions and other collective effects may be important.

Opto-mechanical effects in CNTs have also been observed [22]. Our results allow us to predict strong or weak axial distortions as an elastic response to light, depending on the signs of C_z for electrons and holes. Consider, for instance, electron-hole pairs generated by light in (11,0) and (7,0) CNTs. From the signs of C_z (the same signs of ϵ_z^{max} in Table I), we can see that an electron polaron causes an axial expansion in both (11,0) and (7,0) CNTs. On the other hand, a hole polaron causes an expansion in the (11,0) and a contraction in the (7,0). Therefore, for the (11,0) CNT, the axial mechanical effects of the electron and hole will add up and the CNT will have a strong elastic response to light. On the other hand, electron and hole strains will partly cancel out in the (7,0) CNT, leading to weaker opto-mechanical effects.

In conclusion, we predict the existence of polarons in semiconducting CNTs. Polaron properties are estimated from *ab initio* total-energy calculations for neutral uniformly distorted CNTs within a continuum approach. The complex dependence of polaron signatures on CNT chirality is understood as a combination of classical (elastic) and quantum effects. We show that collective polaron effects may have implications in the context of recently observed electro-mechanical [21] and opto-mechanical [22] activities in CNTs. In particular, we predict the existence of two types of nanotubes regarding their elastic response (strong or weak) to light. A quantitative description of these effects should involve inclusion of collective behavior, inter-tube interactions and electrostatic interactions between electrons and holes should be taken into account into the model calculations.

ACKNOWLEDGMENTS

We acknowledge fruitful discussions with M. S. C. Mazzoni. This work is partially supported by Brazilian agencies Conselho Nacional de Desenvolvimento Científico e Tecnológico (CNPq), Fundação Universitária José Bonifácio (FUJB), Programa de Núcleos de Excelência (PRONEX-MCT), Coordenação de Aperfeiçoamento de Pessoal de Nível Superior (CAPES) and Fundação de Amparo à Pesquisa do Rio de Janeiro (FAPERJ).

REFERENCES

- [1] R. Saito, G. Dresselhaus and M. S. Dresselhaus, *Physical Properties of Carbon Nanotubes*, Imperial College Press (1998).
- [2] M. S. C. Mazzoni and H. Chacham, Phys. Rev. B, **61**, 7312 (2000).
- [3] L. Yang, M. P. Anantram, J. Han and J. P. Lu, Phys. Rev. B, **60**, 13874 (1999).
- [4] C. -J. Park, Y. -H. Kim, K. J. Chang, Phys. Rev. B **60**, 10656 (1999).
- [5] M. S. C. Mazzoni and H. Chacham, Appl. Phys. Lett. **76**, 1561 (2000).
- [6] R. Heyd, A. Charlier and E. McRae, Phys Rev. B **55**, 6820 (1997).
- [7] J. Appel, in *Solid State Physics* **21**, 193, F. Seitz, D. Turnbull and H. Ehrenreich, Editors, (Academic Press, 1968).
- [8] R. E. Peierls, *Quantum Theory of Solids* (Clarendon, Oxford, 1955).
- [9] A. J. Heeger, S. Kivelson, J. R. Schrieffer, W. -P. Su, Rev. Mod. Phys **60**, 781 (1988).
- [10] P. Lammert, P. Zhang, and V. Crespi, Phys. Rev. Lett **84**, 2453 (2000).
- [11] K. Harigaya, Phys. Rev. B **45**, 13676 (1992).
- [12] J. W. Mintmire, B. I. Dunlap, and C. T. White, Phys. Rev. Lett. **68**, 631 (1992).
- [13] R. Saito, M. Fujita, G. Dresselhaus and M. S. Dresselhaus, Phys. Rev. B **46**, 1804 (1992).
- [14] K. Harigaya, Synthetic Metals **56**, 3202 (1993).
- [15] C. C. Chamon, Phys. Rev. B **62** 2806 (2000).
- [16] T. Holstein, Ann. Phys. **8**, 325 (1959).
- [17] D. Sánchez-Portal, P.Ordejón, E. Artacho and J. M. Soler, Int. J. Quantum Chem. **65**, 453 (1997); P.Ordejón, E. Artacho and J. M. Soler, Phys. Rev. B **53**, R10441 (1996).

- [18] D. Sánchez-Portal, E. Artacho, J. M. Soler, A. Rubio and P. Ordejon, Phys. Rev. B **59** 12678 (1999).
- [19] N. Wang, Z. K. Tang, G. D. Li, J. S. Chen, Nature **408** 51 (2000).
- [20] X. Blase, L. X. Benedict, E. L. Shirley, and S. G. Louie, Phys. Rev. Lett. **72**, 1878 (1994).
- [21] R. H. Baughman, C. Cui, A. A. Zakhidov, Z. Iqbal, J. N. Barisci, G. M. Spinks, G. G. Wallace, A. Mazzoldi, D. De Rossi, A. G. Rinzler, O. Jaschinski, S. Roth, and M. Kertesz, Science **284**, 1340 (1999).
- [22] Y. Zhang and S. Iijima, Phys. Rev. Lett. **82**, 3472 (1999).

TABLES

TABLE I. Calculated quantities for a polaron in semiconducting zigzag CNTs.

<i>Parameter</i>	(11,0) CNT		(7,0) CNT	
	electron	hole	electron	hole
λ_r (eV)	0.99	7.30	-5.65	-3.91
λ_z (eV)	-8.29	-2.38	-1.55	7.76
k_r (eV/Å)	605	605	194	194
k_z (eV/Å)	644	644	198	198
k_{rz} (eV/Å)	142	142	78	78
ε (meV)	-7.7×10^{-2}	-7.1×10^{-2}	-3.5×10^{-2}	-2.7×10^{-1}
L (Å)	390	404	586	209
m_{pol}/m_{eff}	1.00020	1.00012	1.00001	1.00221
$\epsilon_r^{(max)}$	-6.291×10^{-6}	-1.684×10^{-5}	1.205×10^{-5}	3.413×10^{-5}
$\epsilon_z^{(max)}$	1.783×10^{-5}	8.212×10^{-6}	9.623×10^{-7}	-5.275×10^{-5}
$ \frac{\Delta\ell/\ell}{\Delta y} $	0.142	0.068	0.074	0.146

FIGURES

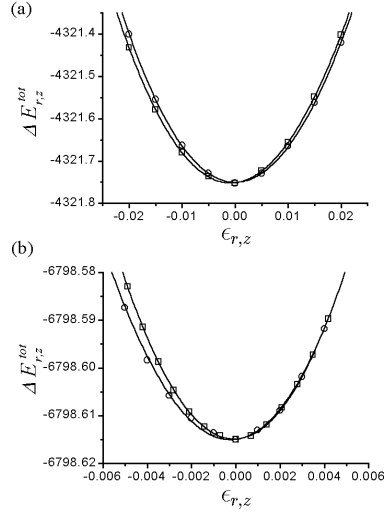


Fig. 1 - Verissimo Alves et al.

FIG. 1. Variation in total energy as a function of ϵ_r (triangles) and ϵ_z (squares) for (a) the (7,0) and (b) the (11,0) CNTs. The solid curve is a 3rd-order polynomial fit to the data. The values of $k_{r,z,rz}$ are obtained from the 2nd derivative of the polynomial at the minimum.

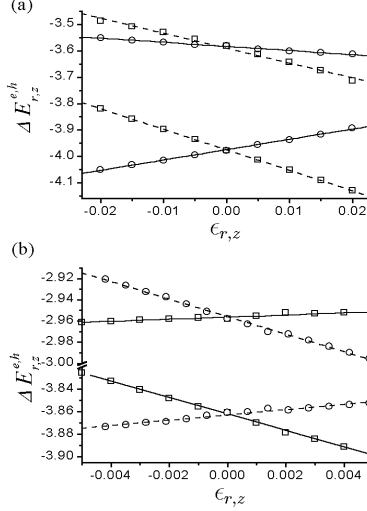


Fig. 2 - Verissimo Alves et al.

FIG. 2. Band edge energies as a function of ϵ_r (squares) and ϵ_z (circles) for (a) the (7,0) and (b) the (11,0) CNT. Data around the regions $\epsilon_{r,z} \simeq 0$ are well fitted by straight lines.